Experimental Evolution Reveals Favored Adaptive Routes to Cell Aggregation in Yeast

Elyse A. Hope, Clara J. Amorosi, Aaron W. Miller,[1] Kolena Dang, Caiti Smukowski Heil, and Maitreya J. Dunham[2]

Department of Genome Sciences, University of Washington School of Medicine, Seattle, Washington 98195

ORCID IDs: 0000-0002-9026-9788 (E.A.H.); 0000-0001-9944-2666 (M.J.D.)

ABSTRACT Yeast flocculation is a community-building cell aggregation trait that is an important mechanism of stress resistance and a useful phenotype for brewers; however, it is also a nuisance in many industrial processes, in clinical settings, and in the laboratory. Chemostat-based evolution experiments are impaired by inadvertent selection for aggregation, which we observe in 35% of populations. These populations provide a testing ground for understanding the breadth of genetic mechanisms *Saccharomyces cerevisiae* uses to flocculate, and which of those mechanisms provide the biggest adaptive advantages. In this study, we employed experimental evolution as a tool to ask whether one or many routes to flocculation are favored, and to engineer a strain with reduced flocculation potential. Using a combination of whole genome sequencing and bulk segregant analysis, we identified causal mutations in 23 independent clones that had evolved cell aggregation during hundreds of generations of chemostat growth. In 12 of those clones, we identified a transposable element insertion in the promoter region of known flocculation gene *FLO1*, and, in an additional five clones, we recovered loss-of-function mutations in transcriptional repressor *TUP1*, which regulates *FLO1* and other related genes. Other causal mutations were found in genes that have not been previously connected to flocculation. Evolving a *flo1* deletion strain revealed that this single deletion reduces flocculation occurrences to 3%, and demonstrated the efficacy of using experimental evolution as a tool to identify and eliminate the primary adaptive routes for undesirable traits.

KEYWORDS flocculation; experimental evolution; yeast, chemostat; *FLO1*

EXPERIMENTAL evolution is an essential tool for investigating adaptive walks, clonal dynamics, competition and fitness, and the genetic underpinnings of complex traits. One question experimental evolution enables us to explore is how often given the same conditions and selective pressures organisms will follow the same adaptive route (Gould's "tape of life") (Gould 1990; Orgogozo 2015). A primary platform for performing evolution experiments in the laboratory is the

chemostat, a continuous culture device invented in 1950 by Monod (1950) and by Novick and Szilard (1950). In a chemostat, new medium is added and diluted at the same rate, maintaining constant growth conditions. Chemostat experiments have provided insight into the mechanisms of genome evolution and adaptation to a variety of selection pressures (Gresham and Hong 2015). However, chemostats have been limited in their utility due in part to frequent selection for biofilms and cell aggregation, which have been observed since the advent of the chemostat. These traits are thought to evolve due to the additional selection imposed for cells that develop a mechanism (*e.g.*, cell–cell or cell–surface adhesion) for reduced dilution and thus increased residence time in the chemostat. In 1964, Munson and Bridges recorded a selective advantage in a bacterial subpopulation that adhered to the wall of a continuous culture device (Munson and Bridges 1964). Topiwala and Hamer followed up on these findings in 1971, and suggested that encouraging this phenotype could actually lead to increased biomass output (Topiwala and Hamer 1971), an idea that has enjoyed

success in subsequent years: chemostats are such a successful system for growing biofilms that they are often used to grow biofilms intentionally by supplying additional substrates to encourage biofilm development (Poltak and Cooper 2011).

In the context of experiments concerning traits unrelated to wall growth and aggregation, however, the ease of biofilm evolution in chemostats represents a significant problem. Since wall growth and aggregation phenotypes develop as an adaptation to the experimental vessel itself, they develop regardless of the intended selective pressures in any given experiment. The evolution of wall growth and cell aggregation inside the continuous culture vessel seeds competing subpopulations, differentially restricting nutrient access for aggregating cells and skewing the likelihood of dilution (Smukalla *et al.* 2008; Fekih-Salem *et al.* 2013)—both variables that should be fixed. Thus, developing a strain with reduced potential for evolving biofilm-related traits in this type of experimental system has many practical benefits.

Combating biofilm-related traits is also important in medicine and industry. Pathogenic yeasts like *Candida albicans* and *Candida glabrata* use the formation of biofilms and filamentous extensions to colonize human tissues, and persist on the surfaces of medical devices such as catheters (Cormack *et al.* 1999; Douglas 2003; Verstrepen and Klis 2006; Nobile and Johnson 2015). *S. cerevisiae* can also act as an opportunistic pathogen in immunocompromised patients (Enache-Angoulvant and Hennequin 2005; Muñoz *et al.* 2005), and the combination of its own virulent potential, its biofilm-forming ability, and its genetic homology with more commonly pathogenic organisms like *C. albicans* and *C. glabrata*, make it a promising model for biofilm formation (Reynolds and Fink 2001). In *S. cerevisiae*, cell-to-cell adhesion is mediated by interactions between lectin-like cell wall proteins in one cell and the cell wall sugars in another (Verstrepen and Klis 2006). This interaction is termed "flocculation," and is a mechanism by which yeast can survive stresses, including treatment from antimicrobial compounds (Stratford 1992; Smukalla *et al.* 2008), with the cells on the interior of the floc physically protected from chemical treatments that more easily kill the outer layer of cells. This protective function is mirrored in pathogenic yeasts: in *C. glabrata*, which causes as many as 15% of fungal infections, and in *C. albicans*, which contributes significantly to sepsis cases, cell wall proteins in the yeast interact with cell wall sugars in human epithelial cells to allow the yeast to directly colonize human tissues using a biofilm-based mechanism (Cormack *et al.* 1999; Nobile and Johnson 2015). Using a model like *S. cerevisiae* to achieve a better understanding of the breadth of biofilm related phenotypes, like flocculation, and their underlying genetics could lead to better methods for testing antimicrobial compounds and designing targeted therapeutics (Ribeiro *et al.* 2016).

In industrial fermentations using *S. cerevisiae*, the stress-resistant properties of flocs can make flocculating strains well suited to harsh industrial conditions (Westman and Franzén 2015). Flocculation also contributes to natural sedimentation that reduces the need to extract yeast from the culture using costly methods such as centrifugation or chemical immobilization. Yeast flocculation is therefore being considered a useful technology to increase the efficiency and decrease the expense of bioethanol production (Sivakumar *et al.* 2010), and an improved understanding of yeast flocculation is important for selecting and designing yeast to use in industrial bioreactors (Domingues *et al.* 2000).

Cell aggregation, which we define here as an umbrella term to include both flocculation and mother/daughter separation defects (Stratford 1992), has dozens of known contributing genes identified by QTL mapping, deletion collection, genetic screen, and linkage analysis studies (Liu *et al.* 1996; Palecek *et al.* 2000; Brem 2002; Verstrepen *et al.* 2005; Borneman *et al.* 2006; Lee *et al.* 2011; Brückner and Mösch 2012; Ryan *et al.* 2012; Granek *et al.* 2013; Roop and Brem 2013; Kim *et al.* 2014; Taylor and Ehrenreich 2014; Cullen 2015; Ratcliff *et al.* 2015; Taylor *et al.* 2016). Our primary interests in this study were to determine, across many evolution experiments, whether the genes involved in the evolution of aggregation were expected or novel, and ascertaining whether all aggregating clones achieved this final phenotype through one primary, or many equally favored, adaptive routes. Given the extensive list of genes involved in aggregation that could potentially contribute to its evolution in a chemostat, this is a particularly promising system for exploring "tape of life" questions due to the large number of possible solutions.

To ask how yeast evolve aggregation, we used multiplexed parallel evolution experiments coupled with genetics and whole genome sequencing to determine the causal mutations in 23 aggregating clones isolated from evolution experiments that ran 300 or more generations. Despite the known genetic complexity of aggregation, most of the causal mutations appeared to operate through a favored adaptive route: activating flocculation gene *FLO1*. Blocking this favored route by deleting *FLO1* significantly reduced incidence of flocculation in further evolution experiments, demonstrating the efficacy and potential of data-driven strain engineering, even for complex traits.

Materials and Methods

Strains and media used in this study

The ancestral strain for all evolved strains used in this study was *S. cerevisiae* laboratory haploid *MAT*a strain FY4 (S288C), and backcrossing experiments were conducted using its isogenic *MAT*α counterpart FY5. Standard growth medium for overnight liquid cultures and agar plates used in this study was yeast extract peptone dextrose (YEPD) medium, with 2% glucose and 1.7% agar for plates. Glucose-limited, sulfate-limited, and phosphate-limited liquid media

and plates were prepared as in Gresham *et al.* (2008), and detailed media recipes are available at http://dunham.gs. washington.edu/protocols.shtml.

To construct a *flo1* knockout strain, KanMX was amplified from the *FLO1* locus in the *flo1* strain from the yeast knockout collection (Giaever *et al.* 2002) using primers CJA009F/R (Supplemental Material, Table S4 in File S2). The PCR reaction was cleaned using a Zymo DNA Clean and Concentrator kit, and DNA concentration was quantified with a Qubit fluorometer. Strain FY4 (S288C) was transformed with 1 µg of the amplicon in 75 µl of 1-step buffer (50% PEG4000 (40% final), 2 M LiAc (0.2 M final), 1 M DTT (100 nM final), salmon sperm carrier DNA) at 42°, and transformants were selected for G418 resistance. The *flo1*::*KanMX* strain was verified using Sanger sequencing.

Multiplexed chemostat evolution experiments

The first set of evolved clones was generated from 96 evolution experiments, conducted with laboratory strain FY4 and designed to evaluate adaptation to nutrient limitation (A.W. M, unpublished data). The experiments were split equally between three nutrient limited conditions—32 each of glucose, sulfate, and phosphate limitation—and organized into six blocks of 16 vessels maintained at 30°. The evolution experiments were set up, and medium was prepared according to Miller *et al.* (2013), with minor modifications. Sampling was conducted daily. The dilution rate was maintained in a target pump setting range of 0.16 and 0.18 vol/hr, and generations elapsed were calculated as (1.44)*(time elapsed)*(dilution rate). Total generations were calculated as the cumulative sum of these individual times. One vessel was lost to pinched pump tubing that obstructed its medium supply, for a final number of 95 evolution experiments. The remaining 95 evolution experiments were terminated at ~300 generations. Throughout the experiment, vessels were monitored for evidence of wall sticking and aggregation, and, in this initial experiment, both traits were scored together. In later experiments, we scored these traits separately; 12/32 phosphate-limited, 18/32 glucose-limited, and 3/31 sulfate-limited populations demonstrated evidence of aggregation or wall sticking, and we selected nine phosphate, 11 glucose, and three sulfate-limited populations for further analysis.

The comparison between *flo1* knockout and wild-type strains was conducted using 64 glucose-limited chemostats run as above. Within each 16-vessel block, wild-type strains and knockout cultures were set up in alternating rows of four. Sampling was conducted once weekly up to 150 generations,. Cultures were monitored daily for evidence of contamination, flocculation, and colonization in any of the media or effluent lines. After 150 generations, samples were stored twice weekly, and microscopy images for all cultures were saved once weekly. At the final timepoint, microscopy images were collected on all cultures. Clumps from the bottom of the culture, or rings adhering to the vessel walls, were collected with long sterile cotton swabs and resuspended in medium

and glycerol for storage. The final populations were plated on YPD to check for contamination, and replica-plated onto G418 to validate the presence of the *KanMX* marker in only the expected *flo1* knockout populations.

Clone isolation

Colonies were struck out from glycerol stocks of the final time point of each experiment, inoculated into liquid culture and grown overnight at 30°. From overnight cultures that displayed a clumping, and/or settling, phenotype, single cells were isolated using micromanipulation on a Nikon Eclipse 50i dissecting microscope, allowed to grow into colonies, screened for the phenotype in an overnight liquid culture of the appropriate nutrient-limited medium, and saved at −80° in glycerol stocks.

Whole genome sequence (WGS) analysis

Genomic DNA for each clone was extracted using a Zymo YeaStar genomic DNA kit, checked for quality using a NanoDrop ND-1000 spectrophotometer, and quantified using an Invitrogen Qubit Fluorometer. Genomic DNA libraries were prepared for Illumina sequencing using the Nextera sample preparation kit (Illumina), and sequenced using 150 bp paired-end reads on an Illumina HiSeq. Ancestral DNA was prepared using a modified Hoffman-Winston preparation (Hoffman and Winston 1987).

Average sequence coverage from WGS of the clones was 97×. The reads were aligned against the genome sequence of sacCer3 using Burrows-Wheeler Aligner version 0.7.3 (Li and Durbin 2009). PCR duplicates were marked using Samblaster version 0.1.22 (Faust and Hall 2014), and indels were realigned using GATK version 3.5 (McKenna *et al.* 2010). For Single Nucleotide Variant (SNV) and small indel analysis, variants were called using the bcftools call command (Li and Durbin 2009). SNVs/indels were filtered for quality and read depth, and mutations unique to the evolved clones were identified, annotated with a custom Python script (Sunshine *et al.* 2015), and verified by visual examination with the Integrative Genomics Viewer (IGV) (Robinson *et al.* 2011). This analysis revealed an average of three high quality SNVs/indels per clone after filtering, with a maximum of 16. Complete sequencing data for all of these clones is available under NCBI BioProject PRJNA339148, BioSample accessions SAMN05729740-5729793. Structural variants were called using lumpy (version accessed on July 6, 2016) (Layer *et al.* 2014), and copy number variants were called using DNAcopy (version accessed on July 21, 2016) (Seshan and Olshen 2015) on 1000 bp windows of coverage across the genome.

The deletion in gene *MIT1* was validated in clones YMD2694 and YMD3102 using PCR (primers EH053PF/PR) (Table S4 in File S2) and Sanger sequencing. Validation of other mutations is described below.

Microscopy and validation of separation defects

Strains were grown overnight in 5 mL YEPD liquid culture at 30°; 5 µl of culture was examined microscopically at

150× magnification, and photographed using a Canon Powershot SD1200 IS digital camera. Images were scored for evidence of mother–daughter separation defects, which were identified in two of the clones: YMD2680 and YMD2689. To validate the separation defects, calcofluor white was added to 1×10^7 cells at a concentration of 100 μg/ml, pipetted to mix, and incubated in the dark for 5 min or more. Cells were pelleted at $16,100 \times g$ for 1 min in an Eppendorf 5415R centrifuge, and the supernatant was removed. The pellet was then washed vigorously with 500 μl water three times, and resuspended in 50 μl water. Bud scars were visualized using a DAPI filter at 630× magnification (Figure S2A in File S1).

To validate true flocculation in the remaining clones, the evolved clones and ancestral strain were inoculated into 100 μl YEPD cultures in two replicates in a round-bottom 96-well plate, and grown overnight at 30° without agitation. Cultures were resuspended by pipetting, and 5 μl of culture was examined microscopically at 150× magnification and imaged. Cells were pelleted, and supernatant removed by pipetting, and one replicate was resuspended in 100 μl water, and the other in 100 μl 4 mM EDTA. Each replicate was pipetted ten times, and then examined microscopically and imaged. After ∼50 min, replicates were resuspended again by pipetting five times, examined microscopically, and imaged again.

Quantitative settling assay

Settling analysis was conducted according to the protocol described in Hope and Dunham (2014). Briefly, each evolved clone or backcross segregant was grown in 5 ml YEPD for 20 hr at 30°; strain YMD2691 and its segregants are slow growing, so an additional replicate was completed for these segregants with 30 hr of growth. Each culture tube was vortexed, and then placed over a black background to settle for 60 min, with photos taken of the settling culture at time zero immediately after vortexing, and at time 60 after 1 hour of settling. Images were converted to black and white in Picasa version 3.9.141.306, and analyzed in ImageJ version 1.47v (Abramoff et al. 2004). The settling ratio (percent of tube cleared at 60 min) was calculated as in Hope and Dunham (2014). Three replicate measurements were taken on each image of the evolved clones, and a single measurement was made for the segregants.

Backcrossing and settling segregation patterns

All clones were backcrossed to strain FY5. An average of 16 full tetrads per cross were dissected, excluding separation defect strains YMD2680 and YMD2689, with additional dissections for crosses with clones YMD2678 (24 tetrads total) and YMD2697 (38 tetrads total). Segregants were inoculated into 100 μl YEPD in round-bottom 96-well plates, and grown overnight at 30° without agitation. Plates were resuspended by gentle pipetting, and allowed to settle without agitation for 15 min, when they were photographed and scored for settling ability.

Complementation testing for separation defects

Clones YMD2680 and YMD2689 were additionally crossed to the ace2 and bem2 null mutants from the yeast knockout collection (Giaever et al. 2002) to reveal the influence of the individual mutations on the original clonal phenotype. Microscopy images of YEPD liquid cultures of three zygotes from each cross, grown overnight, were compared to the phenotypes of the ace2 and bem2 haploid null mutants (Figure S2B in File S1). Additional comparisons were made against homozygous diploid ace2 or bem2 null mutants, created from crosses between the yeast knockout strains and haploid MATa derivatives of the Magic Marker collection (Pan et al. 2004); the MATa strains employed in this cross carry an additional copy of transporter SUL1 unrelated to the phenotype of interest. Zygotes were created by micromanipulating mate pairs due to the separation defect, and all zygotes were verified using a standard halo mating assay (protocol available at http://dunham.gs.washington.edu/protocols.shtml).

Bulk segregant analysis (BSA)

Crosses for clones YMD2684, YMD2686, YMD2687, YMD2696, YMD2697, YMD2698, and YMD2699 were not utilized for BSA after this point as it was determined that they harbored the Ty insertion in the FLO1 promoter; four strains that harbored this insertion (YMD2681, YMD2683, YMD2685, and YMD2690) were included in BSA to verify causality for the Ty insertion. The cross with clone YMD2701 was also not included for BSA because it did not segregate the settling trait 2:2. The nine remaining strains without a FLO1 promoter Ty element insertion or separation defect were analyzed using BSA. Segregants were binned into two pools of cells according to phenotype (settling or nonsettling). Cells were pelleted, washed once with 500 μl water, transferred to a 2 ml lock-top Eppendorf tube, pelleted again, decanted, and frozen at −20° until DNA extraction. Genomic DNA was extracted using a modified Hoffman-Winston preparation (Hoffman and Winston 1987). Sequencing libraries were prepared using Nextera library preparation protocols as described for the original clones.

To identify causal mutations, BSA pools were analyzed similarly to the evolved clones, but filtered individually by sample. For each sample, mutations present in both the settling and nonsettling pool were removed. Mutations present at an allele frequency of one were determined to be causal.

Identification of Ty element insertion location and element type

A Ty insertion in the promoter of FLO1 was identified in 12 of the evolved flocculent clones by visual examination in IGV and split read analysis tool retroSeq (Keane et al. 2013). These insertions were verified as full-length using PCR with primers CJA007F/R (Table S4 in File S2). In some cases, an exact breakpoint was determined using the program lumpy, but, for other samples, the Ty element insertion location was determined by visual examination in IGV. All insertions placed the Ty element in reverse orientation with respect to the FLO1 gene, determined by manual analysis of the mapping orientation of split reads.

A 2.1 kb region upstream of *FLO1*, and including the start of the ORF, was amplified using PCR with Phusion polymerase and primer pair CJA007F/R (Table S4 in File S2) for each clone, with a Ty insertion identified in WGS. The presence of a Ty element insertion leading to a 6 kb expansion was verified on a 1% agarose gel. PCR verification of the insertion failed in three clones, YMD2681, YMD2683, and YMD2697. The PCR reactions were cleaned using a Zymo DNA Clean and Concentrator kit, and eluted in 100 μl of water. Ty1 contains two *Eco*RI sites not shared with Ty2, and Ty2 contains a unique *Bam*HI site missing from Ty1; these features facilitate classification of Ty type by restriction digest. The cleaned amplicons were split into two restriction enzyme digest reactions, one with *Eco*RI and the other with *Bam*HI (New England BioLabs). A model of the amplified region was created in sequence analysis software Ape v2.0.45 (version accessed on July 30, 2012) (Davis 2012), with a Ty insertion in the middle of each hot spot insertion region: Ty insertions were observed between 95 and 156 bp, and between 394 and 470 bp upstream of the *FLO1* ORF, so, for the close insertion model, a Ty1 was added at 125 bp from the ORF, and, for the far insertion model, at 432 bp from the ORF. Predicted cutting with *Eco*RI for the close insertion site yielded four bands at 208, 1408, 2344, and 4118 bp, and for the far insertion site four bands at 208, 1408, 2651, and 3811 bp. We observed the three longest bands as predicted on a 1% agarose gel following the restriction digests, with distinct size differences between the mid and high bands for clones with known close and far insertions; for all evolved clones successfully analyzed, the insertion was classified as a Ty1. Predicted banding patterns for cleavage with *Bam*HI in the region were also consistent with Ty1 elements. As a positive control, a known Ty2 element was amplified from the S288C genome using primers EH054PF/PR (Table S4 in File S2), and the banding patterns that would be present for a Ty2 element with *Bam*HI and *Eco*RI digests were confirmed.

Crosses to determine FLO1 dependence of mutations in ROX3, CSE2, and MIT1

*MAT*α segregants of clones with mutations in *CSE2* (YMD2678), *ROX3* (YMD2691), and *MIT1* (YMD2694) were crossed to a *flo1* knockout strain to facilitate examination of the phenotype of the double mutant progeny, recorded based on the settling ratio of segregants in 16–18 tetrads per cross. Mating types of segregants were verified using a standard halo mating assay (protocol available at http://dunham.gs.washington.edu/protocols.shtml).

Sequencing analyses for secondary modifiers in clones YMD2683 and YMD2690

Two strong candidates for clones with secondary modifiers were YMD2683, with an elongated cell morphology, and YMD2690, with an expansion of the internal repeats in *FLO11*. All of the segregants screened in the quantitative settling assay for clone YMD2683 were also tested for mutations in genes *HSL7*, *IRA1*, *VTS1*, and *TCP1* using primers EH045PF-EH048PR (Table S4 in File S2), and sent for Sanger sequencing by Genewiz.

Microscopy was performed on all of the segregants from the YMD2683 cross, and nine additional segregants were selected based on cell morphology (two with round suspended cells, two with long suspended cells, two with round flocculent cells, and three with long flocculent cells); all were analyzed with the quantitative settling assay and sequenced for mutations in *HSL7* and *IRA1*.

For seven settling segregants from the backcross with clone YMD2690, the *FLO11* internal repeat region was amplified using primers EH030PF/PR (Table S4 in File S2), and results were examined on a 1% agarose gel. For the same segregants, the region of *HOG1* surrounding a premature stop in the clone was amplified using primers EH052PF/PR (Table S4 in File S2), and sent for Sanger sequencing.

Data availability

The authors state that all data necessary for confirming the conclusions presented in the article are represented fully within the article. Data available in public repositories: all of the NCBI BioProject PRJNA339148, BioSample accessions SAMN05729740-5729793.

Results

Experimental evolution studies using continuous culture systems have suffered from small sample sizes in the past, a challenge that has been addressed through our multiplexed miniature chemostat system (Miller *et al.* 2013). In a previous study designed to test changes in fitness in response to different nutrient limitations, we ran 96 miniature chemostats under three different nutrient limitations for 300 generations (A.W.M., unpublished data). We observed that, by 300 generations, 34.7% had gained a visible cell aggregation phenotype not present in the ancestral strain, an S288C derivative that cannot aggregate due to a nonsense mutation in transcription factor Flo8 (Liu *et al.* 1996).

Majority of aggregating clones demonstrate characteristics of true flocculation

We selected clones for further study from the 23 populations with a strong aggregation phenotype. We conducted a number of phenotypic and genotypic analyses on the selected clones in order to determine how each strain had independently evolved the ability to aggregate. We quantified the settling ability of the evolved clones compared to the ancestral strain (Figure 1 and Table S1), a metric that describes the primary phenotype of interest in these experiments. We also examined the cellular morphology of all evolved clones microscopically, and determined that two of the 23 clones (YMD2680 and YMD2689) show a cellular chaining phenotype indicative of a mother–daughter separation defect, while the remaining clones had aggregating round cells characteristic of cell–cell adhesion and true flocculation (Figure S1 in File S1). We confirmed the bud separation defect in YMD2680 and YMD2689 using calcofluor white staining (Figure S2A in File S1), which preferentially stains
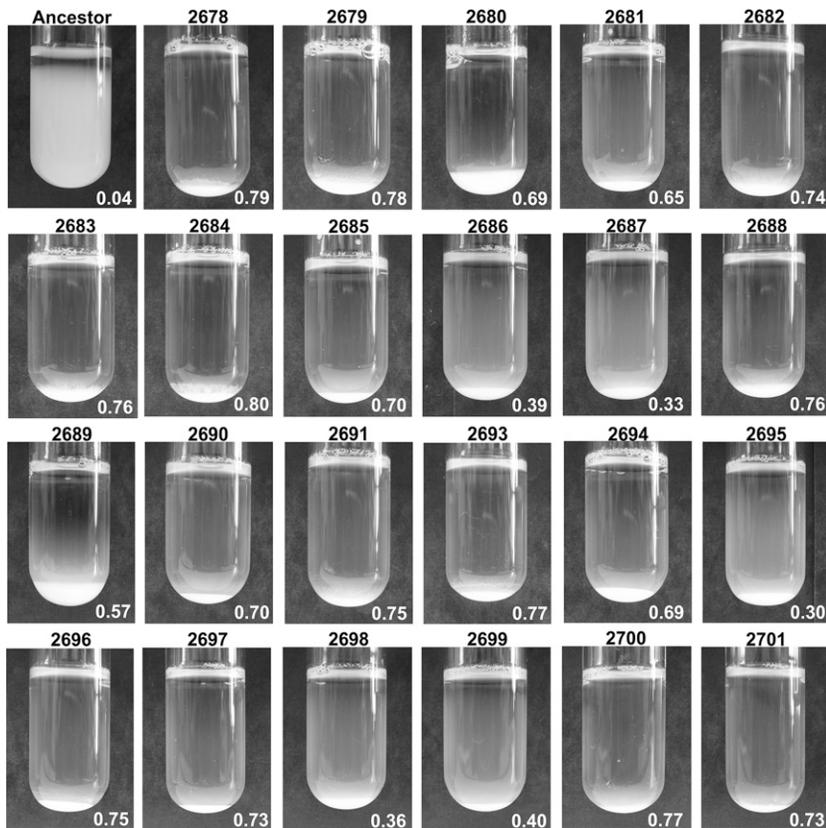
Figure 1 Quantitative settling of aggregating evolved clones. Images of the 60 min settling time point for ancestral strain FY4, and 23 evolved clones with aggregation trait. Cultures were grown to saturation in 5 ml YEPD liquid medium. Settling ratio values are shown in bottom right of each image; ratios are the mean of three measurement replicates on the image shown.

the increased chitin present at yeast bud scars (Pringle 1991). To further distinguish separation defects from flocculation, we treated the evolved clones with a deflocculation buffer containing a chelating agent, EDTA; true flocculation is facilitated by calcium ions and reversible, while separation defects are not (Stratford 1989; Liu *et al.* 1996). We verified that all clones excluding YMD2680 and YMD2689 exhibit true flocculation that is reversible upon treatment with EDTA (Figure S3 in File S1).

Mutations in FLO1 promoter and genes TUP1 and ACE2 are primary adaptive routes to aggregation

We performed WGS on the 23 clones from generation 300 of the evolution experiments, and analyzed the resulting sequence data to identify SNVs, small insertions or deletions (indels), Copy Number Variants (CNVs), and structural variants (Table S2, *Materials and Methods*). We developed a list of candidate genes likely to contribute to the evolution of aggregation phenotypes (Table S3 in File S2) from 17 different papers examining biofilm and cell aggregation related-traits, and several of the SNVs identified in our clones were in candidate genes (*e.g.*, *ACE2*, *HOG1*, and *TUP1*). We did not identify any instances of reversion of the ancestral point mutation in transcription factor gene *FLO8*.

In both clones harboring separation defects, we discovered short insertions and deletions in the transcription factor gene *ACE2*, both of which cause a shift in the reading frame and introduction of a premature stop codon. These results are

consistent with prior literature showing that loss-of-function mutations in this gene cause settling/clumping phenotypes in other experimental evolution scenarios (Voth *et al.* 2005; Koschwanez *et al.* 2013; Oud *et al.* 2013; Ratcliff *et al.* 2015). Furthermore, *ace2* null mutants have the characteristic cell separation defect that we observed in our clones (Libby *et al.* 2014; Ratcliff *et al.* 2015). Using complementation with the wild-type allele, we verified that the *ACE2* mutations were causative of the separation defect aggregation phenotype in these two clones (Table 1), with subtle modification to the cell morphology by *BEM2*—a gene involved in bud emergence that is also mutated in both clones (Figure S2B in File S1) (Bender and Pringle 1991; Kim *et al.* 1994). This type of separation defect in yeast is considered a type of multicellularity, and can be an adaptive trait when cells are challenged with local dispersal of nutrients (Koschwanez *et al.* 2011, 2013), settling (Ratcliff *et al.* 2012, 2013), or, as we show here, residence time in chemostats (Oud *et al.* 2013). We would predict that floc formation could also be an adaptive strategy for cultures evolved under certain stress treatments. Though the goal of our study was to determine how best to avoid the evolution of these phenotypes, chemostats could be a useful selection regime adding to the existing experimental evolution systems that seek to better understand the emergence of multicellularity, biofilms, and related traits.

In the 21 flocculent clones, the most common mutation we identified was a full-length insertion of a yeast transposable (Ty) element in the promoter region of *FLO1*. We saw this

Table 1 Causal mutations for the aggregation phenotype in 23 evolved clones

Clone (YMD)	Nutrient Limitation	Causal Gene	Systematic Name	Mutation Type
2678	G	CSE2	YNR010W	Ty insertion in ORF at R137
2679	S	TUP1	YCR084C	Stop-gained Q181*
2680	G	ACE2	YLR131C	S115 indel (2 bp deletion); premature stop introduced
2681	G	FLO1	YAR050W	Ty in promoter (156 bp upstream of ORF)
2682	P	TUP1	YCR084C	Q107-P143 deletion in ORF (106 bp); premature stop introduced
2683	G	FLO1	YAR050W	Ty in promoter (139 bp)
2684	S	FLO1	YAR050W	Ty in promoter (127 bp)
2685	G	FLO1	YAR050W	Ty in promoter (397 bp)
2686	P	FLO1	YAR050W	Ty in promoter (151 bp)
2687	P	FLO1	YAR050W	Ty in promoter (156 bp)
2688	P	TUP1	YCR084C	Ty insertion in ORF at L341
2689	G	ACE2	YLR131C	L192indel (1 bp insertion); premature stop introduced
2690	G	FLO1	YAR050W	Ty in promoter (449 bp)
2691	G	ROX3	YBL093C	Stop-gained C138*
2693	G	TUP1	YCR084C	Stop-gained Q101*
2694	S	MIT1	YEL007W	L552-M585 deletion in ORF (101 bp); premature stop introduced
2695	P	FLO9	YAL063C	6.2 kb deletion in promoter (229 bp upstream of ORF)
2696	G	FLO1	YAR050W	Ty in promoter (470 bp)
2697	P	FLO1	YAR050W	Ty in promoter (95 bp)
2698	G	FLO1	YAR050W	Ty in promoter (394 bp)
2699	P	FLO1	YAR050W	Ty in promoter (102 bp)
2700	P	TUP1	YCR084C	V592 indel (27 bp deletion); in frame
2701	P	FLO1	YAR050W	Ty in promoter (152 bp)

The gene in which, or in front of which, the causal mutation was found is identified here, along with the type of mutation we recorded. Also shown is the nutrient limitation in which the clones were evolved: G, S, or P for glucose-limited, sulfate-limited, and phosphate-limited, respectively. Positional information about SNVs and indels is exact; other values shown are approximate (*Materials and Methods*).

insertion in 12 of our clones, distributed in two hotspot regions between 95 and 156 bp, and 394 and 470 bp upstream of the *FLO1* start codon (Figure 2, with regulatory information from Basehoar *et al.* 2004; Fichtner *et al.* 2007; Fleming *et al.* 2014). Sequence analysis narrowed the type of Ty element in these insertions to Ty1 or Ty2, and diagnostic PCR and restriction digestion of nine inserts confirmed they were all Ty1 elements. In *FLO1* overexpression, localization, and deletion studies, *FLO1* has been shown to cause flocculation (Bony *et al.* 1998; Guo *et al.* 2000; Smukalla *et al.* 2008); notably, Smukalla *et al.* (2008) demonstrated that GAL-induced expression of *FLO1* in S288C—the background strain for these evolution experiments—induces flocculation, which supports the role we observe for *FLO1* regulation.

In the remaining nine clones, we identified several SNVs and larger insertions and deletions in candidate genes, including *TUP1*, *FLO9*, *IRA1*, and *HOG1*, and many more in noncandidate genes (Table S2 in File S2). Five clones harbored likely loss-of-function mutations in candidate *TUP1*: two stop-gained SNVs in clones YMD2679 and YMD2693; one 27 bp deletion in YMD2700; one 100 bp deletion in YMD2682; and one Ty element insertion in YMD2688. *TUP1* is a general repressor (Carrico and Zitomer 1998; Zhang *et al.* 2002), but also a repressor of *FLO1* (Fleming *et al.* 2014), and loss-of-function mutations in this gene have been associated with

flocculation since 1980 (Stark *et al.* 1980; Lipke and Hull-Pillsbury 1984; Williams and Trumbly 1990; Teunissen *et al.* 1995). The frequently observed mutations in *TUP1* could function to derepress *FLO1* or any number of other candidate genes. In a different clone, YMD2695, we identified a 6.2 kb deletion from 229 bp to 6.4 kb upstream of flocculin gene *FLO9*. We also identified high confidence mutations not previously associated with aggregation in nearly all clones.

BSA verifies causal mutations in novel genes

Because of the number of high confidence mutations in each clone, we could make hypotheses about causality. To test causality, and examine the genetic complexity of the trait in each clone, we turned to a different method: BSA. We backcrossed the 21 evolved flocculent clones to a nonflocculent strain isogenic to the ancestor, but of the opposite mating type. We excluded the two clones with separation defects because their causality was clear, and their budding defect interfered with tetrad dissection. BSA leverages meiotic recombination and independent assortment to link a trait to a causal allele, which will be observed in all progeny with the phenotype of interest. In turn, unlinked noncausal alleles should assort equally between progeny with and without the phenotype (Brauer *et al.* 2006; Segrè *et al.* 2006; Birkeland *et al.* 2010) (Figure 3A). Backcrossing also allowed us to estimate the
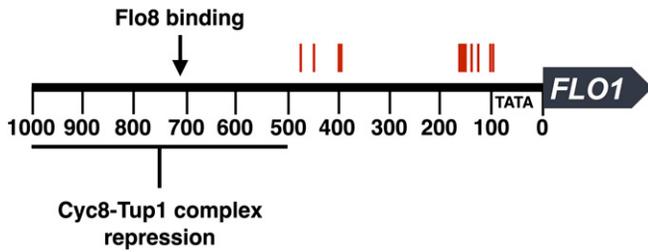
Figure 2 Ty element insertion sites cluster in two regions of the *FLO1* promoter. The region 1 kb upstream of *FLO1* is shown with the insertion site positions of Ty elements observed in 12 evolved clones in red. Locations shown in this figure serve to demonstrate the primary regions of insertion only; for best estimates of exact insertion locations see Table 1. Flo8 binding site and Tup1-Cyc8 repression information adapted from Fichtner *et al.* (2007) and Fleming *et al.* (2014). The TATA box is shown at 96 bp from the start of the open reading frame, as in Basehoar *et al.* (2004).

genetic complexity of the trait: if two of four meiotic progeny have the phenotype and two do not, this indicates a single causal allele for the phenotype. We observed this 2:2 segregation pattern in 20 of the 21 evolved clones, and pooled and sequenced the progeny with and without the trait to identify which of the initial candidate alleles was causal.

We subjected all of our clones with genic mutations, including large insertions and deletions, to BSA analysis, and included four of the clones with a Ty element insertion in the *FLO1* promoter. The analysis pipeline (*Materials and Methods*) identified mutations at 100% frequency in the flocculent pools, and confirmed the causality of the *FLO1*, *TUP1*, *FLO9*, and *ROX3* mutations. BSA also confirmed the causality of mutations in *CSE2* and *MIT1*, genes not previously associated with flocculation (though both have been linked to related traits such as invasive growth and biofilm formation, see below). For the three evolved clones with causal SNVs, the frequency of each candidate in the flocculent and nonflocculent pools is shown in Figure 3, B and C; in each case, the causal mutant allele was at 100% frequency in the flocculent pool. Using the combined results of WGS and BSA, we were able to resolve the causal mutation for all 23 of the evolved clones, with a complete summary of our findings in Table 1.

Functional FLO1 is necessary for flocculation driven by ROX3, CSE2, and MIT1 mutations

Given the large number of potentially activating mutations that we recovered in *FLO1*, we hypothesized that the causal *ROX3* and *CSE2* mutations we recorded also act through *FLO1*, via loss of repression. Several lines of evidence make *ROX3* a reasonable candidate repressor for *FLO1*, and/or other *FLO* genes. Loss-of-function mutations in *ROX3* have been previously associated with flocculation (Brown *et al.* 1995), and also pseudohyphal growth, which is a trait related to haploid invasion and regulated by *FLO* genes (Guo *et al.* 2000). *ROX3* and *CSE2* both encode components of the RNA polymerase II mediator complex, which also includes Sin4, Srb8, and Ssn8, whose role in *FLO* gene repression is
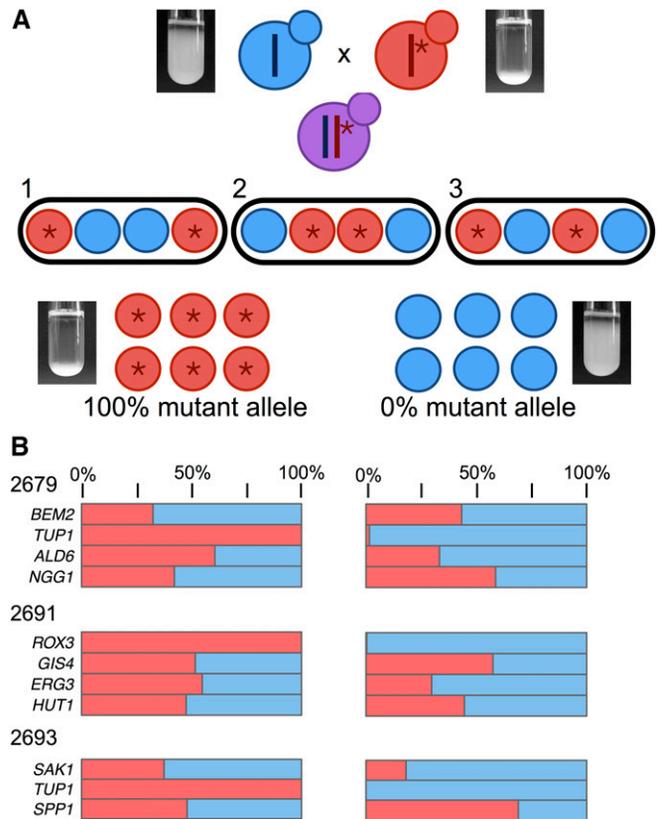

Figure 3 BSA leverages recombination to identify mutations that cosegregate with the flocculation trait. (A) An evolved clone with the phenotype of interest, shown here as settling in liquid culture, is backcrossed to the ancestral strain lacking the phenotype. Dissection of tetrads resulting from this cross reveals the segregation pattern of the trait among meiotic progeny, with 2:2 segregation (two segregants with the settling trait and two without), indicative of single gene control of the trait. Segregants with and without the trait are pooled and sequenced, and alleles that cosegregate with the trait are identified as causal. (B) For three backcrosses, pooled sequencing results are shown for both pools of segregants, those with the settling trait on the left, and without the settling trait on the right. The strain identifier for the evolved clone in the cross is shown on the left, along with a list of candidate genes that had high quality SNV calls in the clone. The red bar shows the % of each of those candidate mutations seen in each pool, with mutations seen at 100% frequency identified as cosegregating with the trait, and therefore causal.

described in Fichtner *et al.* (2007). Mutations in other components of Mediator have previously been shown to cause clumping (Koschwanez *et al.* 2013). In order to test the relationship between the *ROX3* and *CSE2* mutations and *FLO1*, we examined the ratio of settling to nonsettling progeny in crosses between a *flo1* knockout strain, and strains harboring the *CSE2* and *ROX3* causal mutations. For example, 50% settling and 50% nonsettling segregants compiled over all tetrads would indicate that both the *cse2 FLO1* and *cse2 flo1* segregants flocculate, and that the function of the *cse2* mutation is not dependent on a functional *FLO1*, whereas 25% settling and 75% nonsettling segregants, and the presence of tetrads segregating 1:3 and 0:4, would indicate that the double mutant does not flocculate, and a functional *FLO1*

is required for the effect of the *cse2* (or *rox3*) mutation to be observed. We observed that the double mutants show a wild-type, nonflocculent, settling phenotype, *i.e.*, that *flo1* is epistatic to the other mutations. This indicates that *FLO1* is required for these mutations to have an effect, and lends support to the hypothesis that Rox3 and Cse2 function as *FLO1* repressors in the wild-type strain.

Analysis of progeny with a *flo1* null mutation and the *MIT1* allele from YMD2694 revealed similarly that the *MIT1* mutation requires a functional *FLO1* to cause flocculation. *MIT1* is a known transcriptional regulator of flocculin genes *FLO1*, *FLO10*, and *FLO11*, and null mutants of *MIT1* exhibit reductions in hallmark biofilm-related traits, including invasive and psuedohyphal growth and colony complexity (Cain *et al.* 2012), which are related to flocculation in S288C (Liu *et al.* 1996; Fichtner *et al.* 2007). This role of *MIT1* in the literature suggests that the allele we record is not a null allele. If the *MIT1* deletion in YMD2694 generated a null allele, we would expect to see a nonflocculent phenotype, as we confirmed is observed in a *mit1* deletion strain; instead, the evolved allele causes a flocculation phenotype, indicating that it serves in some way to enhance the function of *MIT1*. The phenotype is not dominant, however, suggesting the phenotype does not result from a dominant gain-of-function mutation, but perhaps through a more complex interaction. The deletion itself is out-of-frame, and therefore results in a modified C-terminus of the protein, including a premature stop codon and truncation of the final product. From the extensive literature on the *MIT1* ortholog in *C. albicans*, *WOR1*, we know that DNA binding activity is likely confined to the N-terminal portion of the protein, far from the mutation in this allele of *MIT1*: in *WOR1*, two DNA binding regions in the N-terminal portion of the protein are sufficient for full activity (Lohse *et al.* 2010; Zhang *et al.* 2014). *WOR1* and *MIT1* also both have a self-regulatory mechanism through a positive feedback loop—a potential mechanism for the enhanced function implicated by the mutation we observe (Zordan *et al.* 2006; Cain *et al.* 2012).

Phenotypic variation suggests secondary modifiers influence flocculation

Though we identified the *FLO1* promoter Ty element insertion as the primary causal allele for the aggregation trait in 12 of our clones, we observed variation in the types of flocs produced in our preliminary microscopy of the clones (Figure S1 in File S1), and differences in settling even among all strains with a *FLO1* promoter insertion. These differences were not caused by Ty element direction, proximity, or type: all of the Ty elements we were able to validate with PCR and restriction site polymorphisms were of type Ty1. Secondary genetic modifiers of the flocculation trait are an alternative explanation for this phenotypic variation. To identify strains potentially carrying secondary modifier mutations, we examined the distribution of quantitative settling ratios across a subset of settling segregants for each cross (Figure S4 in File S1 and Table S1). Segregants without a modifier were expected to match the evolved parent settling phenotype, while a distribution of settling abilities would be seen as evidence of a potential modifier (Figure S4 in File S1).

One strong candidate for multiple alleles contributing to the aggregation phenotype was clone YMD2701, the only evolved clone that did not segregate the settling phenotype 2:2 during BSA. Sequencing analysis revealed that this clone does have the *FLO1* promoter Ty1 insertion. We also identified an amplification of chromosome I in this clone, both copies of which have the promoter insertion, indicating that two copies of the causal allele are segregating in this backcross; this genotype is consistent with the segregation pattern we observed (Figure S5 in File S1). Within the segregant settling ratios, however, we did not observe this aneuploidy to be a modifier of the trait (Figure S4 in File S1).

In clone YMD2683, we identified a secondary modifier related to cell morphology. In our initial microscopy (Figure S1 in File S1), we observed that clone YMD2683 had an unusual elongated cell morphology, which we observed segregating in the backcross as well. Microscopy of segregants from this cross revealed four phenotypic classes: round, suspended cells; round, flocculent cells; long, suspended cells; and long, flocculent cells (Figure 4A). Segregants from the backcross involving evolved clone YMD2683 had two different settling ratios, the weaker of which correlated with the round, flocculent morphology, while the stronger settling ratio correlated with the long, flocculent cell morphology (Figure 4, A and C). WGS of the original clone identified high quality SNVs in genes *IRA1*, *HSL7*, *VTS1*, and *TCP1*. PCR and Sanger sequencing of each of these genes in segregants from each phenotypic class revealed cosegregating missense mutations in *HSL7* and *IRA1* in all segregants with the long cell phenotype (examples in Figure 4B), suggesting that one or both of these mutations is functioning as a secondary modifier to enhance the phenotype from the *FLO1* Ty element insertion. *HSL7* and *IRA1* are located only 13 kb apart from each other on chromosome II, indicating that this cosegregation could be due to linkage rather than the contribution of both genes to the trait. Although null mutations in *HSL7* are associated with elongated cell morphology in other common strain backgrounds Σ1278B and W303 (Fujita *et al.* 1999; Kucharczyk *et al.* 1999), this morphological change is not observed in the S288C null mutant (Kucharczyk *et al.* 1999), which we have confirmed using the yeast knockout collection (Giaever *et al.* 2002). The S288C background of this evolved strain therefore makes *IRA1* the more likely modifier, though the phenotype could also require both mutations.

Another promising candidate for a secondary modifier was clone YMD2690: segregants from the backcross with this clone showed considerable variation in settling ratios, and the clone harbored a premature stop codon in candidate gene *HOG1* (Table S2 in File S2), although a Ty element in the *FLO1* promoter was identified as the primary causal mutation. Using Sanger sequencing of settling segregants, we determined that *HOG1* was not a secondary modifier of the trait. We conducted additional testing using primers from Zara *et al.* (2009) (Table S4 in File S2) to target the repeat region in flocculin gene
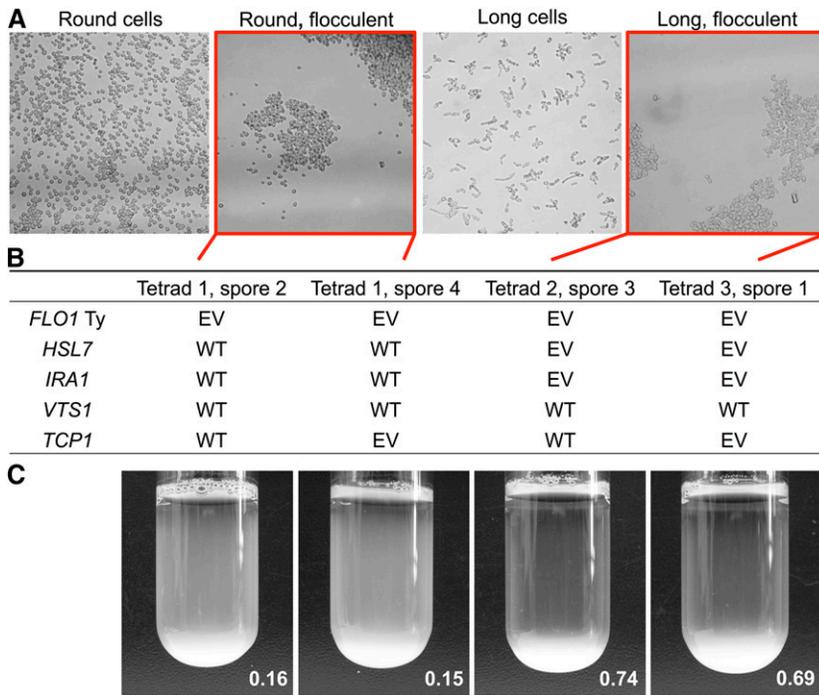
Figure 4 Evolved clone exhibits morphology-related secondary modifier of flocculation phenotype. (A) Meiotic segregants show four phenotypic classes combining morphology and flocculation. Micrographs received additional processing (gray scale conversion, 20% increase in brightness, 20% increase in contrast) to better highlight the phenotypes. (B) Sequencing results for four example flocculent segregants are shown, from two of the phenotypic classes in 4A: two segregants have round flocculent cells, and two have long flocculent cells. All segregants have the *FLO1* Ty insertion. The four candidate SNVs from the evolved clone were Sanger sequenced in the flocculent progeny and the match to the WT (S288C reference) or mutant/evolved base (EV) is recorded. (C) Settling images and ratios for the four flocculent segregants that provided the sequencing data in (B).

FLO11 in clone YMD2690, and found evidence in this clone of a *FLO11* repeat expansion of ∼1 kb in length. All flocculin genes have long arrays of internal tandem repeats (Verstrepen *et al.* 2005); expansions of the internal repeats in *FLO11* have been shown to cause phenotypic variability in biofilm-related traits, and natural isolates of yeast exhibit significant variation in the copy number of the repeats (Fidalgo *et al.* 2008; Zara *et al.* 2009). However, this expansion also did not correlate with variations in strength of the segregant settling ratios, demonstrating that the presence of the *FLO11* expansion in addition to the Ty element insertion did not significantly affect the strength of the phenotype. PCR of all of the evolved clones revealed that only this clone had any evidence of repeat expansion in *FLO11*.

Deleting FLO1 increases time to evolve flocculation and reveals alternate adaptive routes

The results of our analyses of the evolved clones demonstrate a clear role for *FLO1* in the evolution of flocculation; not only do we see changes in the *FLO1* promoter, many of the other mutations we recorded are also in genes encoding proteins that function to regulate *FLO1* (*TUP1*) or participate in complexes that regulate *FLO1* (*ROX3*, *CSE2*). We hypothesized that changes in the regulation of *FLO1* cause the flocculation phenotype in nearly all of the evolved clones, and that deleting *FLO1* would be a promising route for slowing the evolution of flocculation. Deleting a combination of *FLO* genes has been previously employed as a method to try to make laboratory strains easier to work with over long-term experimental evolution (Voordeckers and Verstrepen 2015), and modification of the *FLO1* promoter has been effectively employed in biological circuits controlling flocculation (Ellis *et al.* 2009); however, it is unknown if specifically deleting *FLO1* would be effective on its own. We constructed a *flo1*

strain, and evolved 32 chemostat vessels of wild type, concurrently with 32 chemostat vessels of the *flo1* knockout strain, in glucose limited medium, for >250 generations. Two knockout and one wild-type vessel were lost to contamination after generation 200.

We monitored all vessels for evidence of aggregation, and recorded eight wild-type and one knockout strain that developed aggregation during the course of the experiment, a statistically significant reduction ($P = 0.01$, Fisher's Exact Test). In order to determine the mechanism of the single aggregating *flo1* population, we performed WGS of a clone, and found a Ty element insertion in the promoter of *FLO9*. In addition to the single knockout clone, we sequenced four wild-type strains that also evolved aggregation in the course of the experiment. Two of these harbored *FLO1* promoter Ty element insertions; another had a stop-gained mutation in *NCP1* that has not been verified as causal; and another had a deletion in *MIT1* exactly matching the deletion identified in the clone from the previous series of evolution experiments.

FLO1 deletion does not affect rate of evolution for unrelated traits

We expected that deleting *FLO1* would not impact the rate of evolution for unrelated traits, including wall sticking and separation defects—two other traits we monitored during the knockout evolution experiments. Cell-surface adhesion traits are more often associated with expression of *FLO11* (Guo *et al.* 2000; Verstrepen and Klis 2006), and we would not expect the frequency of evolving separation defects to be affected by changes to flocculation genes. For 32 of the vessels across both genotypes, we recorded the occurrence of some amount of wall sticking 2 days before the final time point; eight of these we recorded as strong wall growth at the

final evolution time point. The strong wall growth observations were split equally between WT and *flo1* knockout populations. Similarly, for mother–daughter separation defects, which we observed through microscopy of each of the final evolution time points, we recorded 12 strains with separation defects, five from the wild type, and six from the knockout evolution experiments, with an additional wild-type strain with an inconclusive microscopy phenotype (Figure S6 in File S1).

To explore the genetic origins of the wall sticking trait, we isolated clones with a strong wall sticking phenotype from six different populations, four from knockout experiments, and two from wild-type experiments. Under the microscope, we observed that all six wall sticking clones harbored a separation defect. To determine if these were all caused by loss of function alleles of *ACE2*, we performed a complementation test using the *ace2* strain from the yeast deletion collection (Giaever *et al.* 2002). We determined that a loss-of-function mutation in *ACE2* was responsible for both the wall sticking and mother–daughter separation defects in five of the six clones. Despite this relationship, we did not observe a strong connection between wall sticking and separation defects on the population level, with 10 strains having only a separation defect, five having only strong wall growth, and only four populations having both phenotypes. The mechanism by which loss of function in *ACE2* facilitates wall sticking remains undetermined.

Discussion

Previous studies have successfully leveraged experimental evolution to understand the genetic contributors to complex traits (Brown *et al.* 1998; Leu and Murray 2006; Hong and Gresham 2014; Voordeckers and Verstrepen 2015). Evolution experiments have also contributed significantly to our understanding of how genomes evolve, and the types of mutations typically observed in yeast grown in chemostats, including SNVs, CNVs, aneuploidy, and transposable element insertions (Adams and Oeller 1986; Dunham *et al.* 2002; Adams 2004; Gresham *et al.* 2008; Araya *et al.* 2010). In our study, we built on these concepts to identify the mutations contributing most to the evolution of cell aggregation—an industrially and medically relevant trait, in addition to a practically useful one for facilitating laboratory work. We determined that in experimental evolution in continuous culture, loss-of-function mutations in *ACE2* are the most common contributors to the evolution of mother–daughter separation defects and wall growth, and mutations that change the regulation of *FLO1* are the most common evolutionary route to flocculation. The majority of causal mutations identified in this study occurred in candidate genes selected for involvement in aggregation traits based on previous literature, but two of the causal mutations were in genes not previously associated with flocculation (*CSE2*, *MIT1*). Both our identification of new genetic associations with flocculation, and of one favored adaptive route to flocculation, demonstrate the efficacy of using experimental evolution as a tool to better understand important complex traits.

This study also demonstrates the power of evolution experiments to determine which genes, among the many genes that are associated with complex traits like flocculation, most frequently contribute to adaptation under specific constraints. Despite the many possible candidates, we saw few of those genes identified in the evolved clones in this study. The genomic context of the laboratory strain could have contributed to this finding; by evolving a strain with a nonsense mutation in flocculation transcription factor Flo8, we were functionally screening for bypass suppressors. A different genetic background might be more likely to reveal different favored adaptations for both flocculation and multicellular phenotypes, and recent work has demonstrated the important role of background in *FLO1* performance during fermentation (Deed *et al.* 2017). Despite the constraint provided by strain background, our findings are in keeping with other work in eukaryotes demonstrating favored adaptive responses, not just in the clear relationships between nutrient limitation and the amplification of nutrient transporters (Brown, Todd, and Rosenzweig 1998; Gresham *et al.* 2008), but also in response to stress treatments. In a more saturated screen, we might start to see contributions from other candidate genes or pathways, but large screens have also revealed parallel adaptation. A study of 240 yeast strains under selective pressure from the antibiotic Nystatin revealed significant parallelism in mutational response through a single pathway (Gerstein *et al.* 2012) similar to the parallelism we discovered through *FLO1* regulation.

An analysis of the population-level data from this and earlier time points will also likely reveal other adaptively beneficial mutations that might have represented viable routes had the *FLO1* promoter mutation been absent. There are promising future opportunities to track the prevalence of individual alleles of interest over time using a targeted deep sequencing platform, such as FREQ-Seq (Chubiz *et al.* 2012). There is also potential to explore the role of experimental conditions and the interplay between nutrient limitation adaptations and aggregation adaptations. In our evolved clones, we recorded many fewer instances of aggregation or wall sticking in sulfate-limited evolution experiments (3/31) than in glucose- or phosphate-limited experiments (18/32 and 12/32, respectively). We hypothesize that decreased likelihood of developing aggregation in sulfate-limited medium is related to the well-documented existence of a rapid and effective adaptive mechanism to sulfate-limited growth via the amplification of a high-affinity sulfate transporter (Gresham *et al.* 2008; Payen *et al.* 2014), which, for sulfate-limited strains, might be more advantageous than aggregation. Indeed, we recorded an amplification of this transporter, *SUL1*, in one of the aggregating strains (YMD2694, with *MIT1* casual allele), which might not affect the aggregation phenotype, but likely affects fitness. The role of other candidate genes that may contribute to flocculation-driven or nutrient limitation-driven evolutionary success might also be revealed in a scenario in which an engineered strain has

been modified to take away the primary adaptive routes we observed.

The primary mechanism of evolution we observed, a Ty element insertion in the *FLO1* promoter region, likely activates *FLO1* expression similarly to previous Ty element systems (Rothstein and Sherman 1980; Errede *et al.* 1984; Coney and Roeder 1988). The reverse orientation of the Ty element with respect to the open reading frame that we observed in all of our clones is the most common activating arrangement (Boeke and Sandmeyer 1991; Servant, Pennetier, and Lesage 2008), and the role of transposable elements in driving adaptive mutations has been well documented in yeast and other organisms (Chao *et al.* 1983; Wilke and Adams 1992; Tenaillon *et al.* 2016). Despite discovering one primary mechanism for evolving flocculation, we also show evidence for other genetic contributors modifying and enhancing the phenotype we observe. There is quantitative variation among settling segregants from crosses with our evolved clones (Figure S4 in File S1), particularly among strains with the *FLO1* promoter Ty element insertion, and we confirmed one example of a secondary modifier of the settling trait in clone YMD2683, in which a change in cell morphology enhanced the trait from the *FLO1* promoter Ty element insertion. Across other clones with trait variation there is potential to discover additional modifiers, both in the form of known candidate genes, including other *FLO* genes with internal tandem repeats, and in genes that have not previously been associated with flocculation.

Each causal mutation in our clones represents a new possible avenue for engineering to reduce aggregation. These could be simple changes, such as fusing genes like *ACE2* and *TUP1*, which frequently acquire loss-of-function mutations, to essential genes, or increasing their copy number or strain ploidy to increase the likelihood of "masking" deleterious recessive mutations (Otto and Goldstein 1992). They can also be iterative: deleting *FLO9* in the *flo1* background could reduce evolution of flocculation even further. Alternative strategies include reducing the mutation rate of these undesirable mutations. The frequency at which we observe activating Ty elements driving flocculation also suggests that future experiments aimed at reducing Ty element expression or mobility could be fruitful. Promising routes for reducing the Ty burden in evolution experiments include inhibiting Ty1 transposition (Xu and Boeke 1991) or utilizing different background strains. There is evidence that strain background contributes significantly to the likelihood of evolving flocculation in chemostat experiments. *Saccharomyces uvarum*, a budding yeast related to *S. cerevisiae* and often used in interspecific hybrid studies, has only Ty4 elements in its genome (Liti *et al.* 2005), and evolves flocculation more slowly than *S. cerevisiae* in chemostat experiments (Heil *et al.* 2017; Sanchez *et al.* 2017). Not only do different species of yeast have different Ty element burdens, natural isolates of *S. cerevisiae* also provide strain-specific differences in Ty ele-

ment burden (Dunn *et al.* 2012; Bleykasten-Grosshans *et al.* 2013), and a reservoir of variation in evolutionary potential that will be useful in future evolution experiments for studying flocculation and other complex traits.

Over the past six decades, experimental evolution in chemostats with yeast and bacteria has provided valuable insights into evolutionary dynamics, and has proven to be a powerful tool for understanding complex traits. Now, with the advent of modern sequencing technology and common strain engineering methods, experimental evolution represents a promising direction for designing and testing strains with reduced (or increased) evolutionary potential. Evolution is gaining popularity as a tool for engineering: as just a few examples, in 2002, Yokobayashi *et al.* (2002) used directed evolution to improve the function of a rationally designed circuit driving a fluorescent reporter, and evolutionary engineering is commonly used to improve carbon source utilization of industrial strains (Garcia Sanchez *et al.* 2010; Shen *et al.* 2012; Zhou *et al.* 2012). Evolution poses a challenge to strain engineering as well: loss, change, and breakage of engineered pathways confounds consistent usage (Renda *et al.* 2014). Our study employs experimental evolution as a tool for engineering, but as a method both to design and to test new strains. We utilized evolution experiments as a means both to discover the genetic underpinnings of a complex trait with real-world applications, and to determine and eliminate the most successful adaptive route in order to generate a more amenable strain background for future experiments. This approach represents a promising engineering technique, not just for flocculation and related traits, but also for traits such as antimicrobial resistance, which represent major challenges of our time.

Literature Cited

Abramoff, M. D., P. J. Magalhães, and S. J. Ram, 2004 Image processing with ImageJ. Biophoton. Int. 11: 36–42.

Adams, J., 2004 Microbial evolution in laboratory environments. Res. Microbiol. 155: 311–318.

Adams, J., and P. W. Oeller, 1986 Structure of evolving populations of *Saccharomyces cerevisiae*: adaptive changes are frequently associated with sequence alterations involving mobile elements belonging to the Ty family. Proc. Natl. Acad. Sci. USA 83: 7124–7127.

Araya, C. L., C. Payen, M. J. Dunham, and S. Fields, 2010 Whole-genome sequencing of a laboratory-evolved yeast strain. BMC Genomics 11: 88.

Basehoar, A. D., S. J. Zanton, and B. F. Pugh, 2004 Identification and distinct regulation of yeast TATA box-containing genes. Cell 116: 699–709.

Bender, A., and J. R. Pringle, 1991 Use of a screen for synthetic lethal and multicopy suppressee mutants to identify two new genes involved in morphogenesis in *Saccharomyces cerevisiae*. Mol. Cell. Biol. 11: 1295–1305.

Birkeland, S. R., N. Jin, A. C. Ozdemir, R. H. Lyons, L. S. Weisman et al., 2010 Discovery of mutations in *Saccharomyces cerevisiae* by pooled linkage analysis and whole-genome sequencing. Genetics 186: 1127–1137.

Bleykasten-Grosshans, C., A. Friedrich, and J. Schacherer, 2013 Genome-wide analysis of intraspecific transposon diversity in yeast. BMC Genomics 14: 399.

Boeke, J. D., and S. Sandmeyer, 1991 4 yeast transposable elements. Cold Spring Harbor Monograph Archive, North America, 21A. Available at: https://cshmonographs.org/index.php/monographs/article/view/3183. Accessed September 13, 2016.

Bony, M., P. Barre, and B. Blondin, 1998 Distribution of the flocculation protein, Flop, at the cell surface during yeast growth: the availability of Flop determines the flocculation level. Yeast 14: 25–35.

Borneman, A. R., J. A. Leigh-Bell, H. Yu, P. Bertone, M. Gerstein et al., 2006 Target hub proteins serve as master regulators of development in yeast. Genes Dev. 20: 435–448.

Brauer, M. J., C. M. Christianson, D. A. Pai, and M. J. Dunham, 2006 Mapping novel traits by array-assisted bulk segregant analysis in *Saccharomyces cerevisiae*. Genetics 173: 1813–1816.

Brem, R. B., 2002 Genetic dissection of transcriptional regulation in budding yeast. Science 296: 752–755.

Brown, C. J., K. M. Todd, and R. F. Rosenzweig, 1998 Multiple duplications of yeast hexose transport genes in response to selection in a glucose-limited environment. Mol. Biol. Evol. 15: 931–942.

Brown, T. A., C. Evangelista, and B. L. Trumpower, 1995 Regulation of nuclear genes encoding mitochondrial proteins in *Saccharomyces cerevisiae*. J. Bacteriol. 177: 6836–6843.

Brückner, S., and H.-U. Mösch, 2012 Choosing the right lifestyle: adhesion and development in *Saccharomyces cerevisiae*. FEMS Microbiol. Rev. 36: 25–58.

Cain, C. W., M. B. Lohse, O. R. Homann, A. Sil, and A. D. Johnson, 2012 A conserved transcriptional regulator governs fungal morphology in widely diverged species. Genetics 190: 511–521.

Carrico, P. M., and R. S. Zitomer, 1998 Mutational analysis of the Tup1 general repressor of yeast. Genetics 148: 637–644.

Chao, L., C. Vargas, B. B. Spear, and E. C. Cox, 1983 Transposable elements as mutator genes in evolution. Nature 303: 633–635.

Chubiz, L. M., M.-C. Lee, N. F. Delaney, and C. J. Marx, 2012 FREQ-Seq: a rapid, cost-effective, sequencing-based method to determine allele frequencies directly from mixed populations. PLoS One 7: e47959.

Coney, L. R., and G. S. Roeder, 1988 Control of yeast gene expression by transposable elements: maximum expression requires a functional Ty activator sequence and a defective Ty promoter. Mol. Cell. Biol. 8: 4009–4017.

Cormack, B. P., N. Ghori, and S. Falkow, 1999 An adhesin of the yeast pathogen *Candida glabrata* mediating adherence to human epithelial cells. Science 285: 578–582.

Cullen, P. J., 2015 Evaluating the activity of the filamentous growth MAPK pathway in yeast. Cold Spring Harb. Protoc. 2015: 276–283.

Davis, M. W., 2012 ApE - A plasmid editor. Available at: http://biologylabs.utah.edu/jorgensen/wayned/ape/.

Deed R. C., B. Fedrizzi, and R. C. Gardner, 2017 *Saccharomyces cerevisiae FLO1* gene demonstrates genetic linkage to increased fermentation rate at low temperatures. G3 (Bethesda) 7: 1039–1048. g3.116.037630.

Domingues, L., A. A. Vicente, N. Lima, and J. A. Teixeira, 2000 Applications of yeast flocculation in biotechnological processes. Biotechnol. Bioprocess Eng.; BBE 5: 288–305.

Douglas, L. J., 2003 *Candida* biofilms and their role in infection. Trends Microbiol. 11: 30–36.

Dunham, M. J., H. Badrane, T. Ferea, J. Adams, P. O. Brown et al., 2002 Characteristic genome rearrangements in experimental evolution of *Saccharomyces cerevisiae*. Proc. Natl. Acad. Sci. USA 99: 16144–16149.

Dunn, B., C. Richter, D. J. Kvitek, T. Pugh, and G. Sherlock, 2012 Analysis of the *Saccharomyces cerevisiae* pan-genome reveals a pool of copy number variants distributed in diverse yeast strains from differing industrial environments. Genome Res. 22: 908–924.

Ellis, T., X. Wang, and J. J. Collins, 2009 Diversity-based, model-guided construction of synthetic gene networks with predicted functions. Nat. Biotechnol. 27: 465–471.

Enache-Angoulvant, A., and C. Hennequin, 2005 Invasive *Saccharomyces* infection: a comprehensive review. Clin. Infect. Dis. 41: 1559–1568.

Errede, B., T. S. Cardillo, M. A. Teague, and F. Sherman, 1984 Identification of regulatory regions within the Ty1 transposable element that regulate iso-2-cytochrome c production in the *CYC7–H2* yeast mutant. Mol. Cell. Biol. 4: 1393–1401.

Faust, G. G., and I. M. Hall, 2014 SAMBLASTER: fast duplicate marking and structural variant read extraction. Bioinformatics 30: 2503–2505.

Fekih-Salem, R., J. Harmand, C. Lobry, A. Rapaport, and T. Sari, 2013 Extensions of the chemostat model with flocculation. J. Math. Anal. Appl. 397: 292–306.

Fichtner, L., F. Schulze, and G. H. Braus, 2007 Differential Flo8p-dependent regulation of *FLO1* and *FLO11* for cell–cell and cell–substrate adherence of *S. cerevisiae* S288c. Mol. Microbiol. 66: 1276–1289.

Fidalgo, M., R. R. Barrales, and J. Jimenez, 2008 Coding repeat instability in the *FLO11* gene of *Saccharomyces* yeasts. Yeast 25: 879–889.

Fleming, A. B., S. Beggs, M. Church, Y. Tsukihashi, and S. Pennings, 2014 The yeast Cyc8–Tup1 complex cooperates with Hda1p and Rpd3p histone deacetylases to robustly repress transcription of the subtelomeric *FLO1* gene. Biochim. Biophys. Acta. Gene Regul. Mech. 1839: 1242–1255.

Fujita, A., A. Tonouchi, T. Hiroko, F. Inose, T. Nagashima et al., 1999 Hsl7p, a negative regulator of Ste20p protein kinase in the *Saccharomyces cerevisiae* filamentous growth-signaling pathway. Proc. Natl. Acad. Sci. USA 96: 8522–8527.

Garcia Sanchez, R., K. Karhumaa, C. Fonseca, V. Sànchez Nogué, J. R. Almeida et al., 2010 Improved xylose and arabinose utilization by an industrial recombinant *Saccharomyces cerevisiae* strain using evolutionary engineering. Biotechnol. Biofuels 3: 13.

Gerstein, A. C., D. S. Lo, and S. P. Otto, 2002 Parallel Genetic Changes and Nonparallel Gene–Environment Interactions Characterize the Evolution of Drug Resistance in Yeast. Genetics 192: 241–252.

Giaever, G., A. M. Chu, L. Ni, C. Connelly, L. Riles *et al.*, 2002 Functional profiling of the *Saccharomyces cerevisiae* genome. Nature 418: 387–391.

Gould, S. J., 1990 *Wonderful Life: The Burgess Shale and the Nature of History*. W. W. Norton & Company, New York.

Granek, J. A., D. Murray, Ö. Kayrkçi, and P. M. Magwene, 2013 The genetic architecture of biofilm formation in a clinical isolate of *Saccharomyces cerevisiae*. Genetics 193: 587–600.

Gresham, D., M. M. Desai, C. M. Tucker, H. T. Jenq, D. A. Pai *et al.*, 2008 The repertoire and dynamics of evolutionary adaptations to controlled nutrient-limited environments in yeast. PLoS Genet. 4: e1000303.

Gresham, D., and J. Hong, 2015 The functional basis of adaptive evolution in chemostats. FEMS Microbiol. Rev. 39: 2–16.

Guo, B., C. A. Styles, Q. Feng, and G. R. Fink, 2000 A *Saccharomyces* gene family involved in invasive growth, cell–cell adhesion, and mating. Proc. Natl. Acad. Sci. USA 97: 12158–12163.

Heil, C. S. S., C. G. DeSevo, D. A. Pai, C. M. Tucker, M. L. Hoang *et al.*, 2017 Loss of heterozygosity drives adaptation in hybrid yeast. Mol. Biol. Evol. (in press).

Hoffman, C. S., and F. Winston, 1987 A ten-minute DNA preparation from yeast efficiently releases autonomous plasmids for transformation of *Escherichia coli*. Gene 57: 267–272.

Hong, J., and D. Gresham, 2014 Molecular specificity, convergence and constraint shape adaptive evolution in nutrient-poor environments. PLoS Genet. 10: e1004041.

Hope, E. A., and M. J. Dunham, 2014 Ploidy-regulated variation in biofilm-related phenotypes in natural isolates of *Saccharomyces cerevisiae*. G3 (Bethesda) 4: 1773–1786.

Keane, T. M., K. Wong, and D. J. Adams, 2013 RetroSeq: transposable element discovery from next-generation sequencing data. Bioinformatics 29: 389–390.

Kim, H. Y., S. B. Lee, H. S. Kang, G. T. Oh, and T. Kim, 2014 Two distinct domains of Flo8 activator mediates its role in transcriptional activation and the physical interaction with Mss11. Biochem. Biophys. Res. Commun. 449: 202–207.

Kim, Y.-J., L. Francisco, G.-C. Chen, E. Marcotte, and C. S. M. Chan, 1994 Control of cellular morphogenesis by the Ip12/Bem2 GTPase-activating protein: possible role of protein phosphorylation. J. Cell Biol. 127: 1381–1394.

Koschwanez, J. H., K. R. Foster, and A. W. Murray, 2011 Sucrose utilization in budding yeast as a model for the origin of undifferentiated multicellularity. PLoS Biol. 9: e1001122.

Koschwanez, J. H., K. R. Foster, and A. W. Murray, 2013 Improved use of a public good selects for the evolution of undifferentiated multicellularity. Elife 2: e00367.

Kucharczyk, R., R. Gromadka, A. Migdalski, P. P. Słonimski, and J. Rytka, 1999 Disruption of six novel yeast genes located on chromosome II reveals one gene essential for vegetative growth and two required for sporulation and conferring hypersensitivity to various chemicals. Yeast 15: 987–1000.

Layer, R. M., C. Chiang, A. R. Quinlan, and I. M. Hall, 2014 LUMPY: a probabilistic framework for structural variant discovery. Genome Biol. 15: R84.

Lee, H. N., P. M. Magwene, and R. B. Brem, 2011 Natural variation in *CDC28* underlies morphological phenotypes in an environmental yeast isolate. Genetics 188: 723–730.

Leu, J.-Y., and A. W. Murray, 2006 Experimental evolution of mating discrimination in budding yeast. Curr. Biol. 16: 280–286.

Li, H., and R. Durbin, 2009 Fast and accurate short read alignment with Burrows–Wheeler transform. Bioinformatics 25: 1754–1760.

Libby, E., W. Ratcliff, M. Travisano, and B. Kerr, 2014 Geometry shapes evolution of early multicellularity. PLoS Comput. Biol. 10: e1003803.

Lipke, P. N., and C. Hull-Pillsbury, 1984 Flocculation of *Saccharomyces cerevisiae tup1* mutants. J. Bacteriol. 159: 797–799.

Liti, G., A. Peruffo, S. A. James, I. N. Roberts, and E. J. Louis, 2005 Inferences of evolutionary relationships from a population survey of LTR-retrotransposons and telomeric-associated sequences in the *Saccharomyces sensu stricto* complex. Yeast 22: 177–192.

Liu, H., C. A. Styles, and G. R. Fink, 1996 *Saccharomyces cerevisiae* S288c has a mutation in *FLO8*, a gene required for filamentous growth. Genetics 144: 967–978.

Lohse, M. B., R. E. Zordan, C. W. Cain, and A. D. Johnson, 2010 Distinct class of DNA-binding domains is exemplified by a master regulator of phenotypic switching in *Candida albicans*. Proc. Natl. Acad. Sci. USA 107: 14105–14110.

McKenna, A., M. Hanna, E. Banks, A. Sivachenko, K. Cibulskis *et al.*, 2010 The genome analysis toolkit: a mapreduce framework for analyzing next-generation DNA sequencing data. Genome Res. 20: 1297–1303.

Miller, A. W., C. Befort, E. O. Kerr, and M. J. Dunham, 2013 Design and use of multiplexed chemostat arrays. J. Vis. Exp. 23: e50262.

Monod, J., 1950 Technique, theory and applications of continuous culture. Ann. Inst. Pasteur (Paris) 79: 390–410.

Muñoz, P., E. Bouza, M. Cuenca-Estrella, J. M. Eiros, M. J. Pérez *et al.*, 2005 *Saccharomyces cerevisiae* fungemia: an emerging infectious disease. Clin. Infect. Dis. 40: 1625–1634.

Munson, R. J., and B. A. Bridges, 1964 "Take-over"—an unusual selection process in steady-state cultures of *Escherichia coli*. Microbiology 37: 411–418.

Nobile, C. J., and A. D. Johnson, 2015 *Candida albicans* biofilms and human disease. Annu. Rev. Microbiol. 69: 71–92.

Novick, A., and L. Szilard, 1950 Description of the chemostat. Science 112: 715–716.

Orgogozo, V., 2015 Replaying the tape of life in the twenty-first century. Interface Focus 5: 20150057.

Otto, S. P., and D. B. Goldstein, 1992 Recombination and the evolution of diploidy. Genetics 131: 745–751.

Oud, B., V. Guadalupe-Medina, J. F. Nijkamp, D. de Ridder, J. T. Pronk *et al.*, 2013 Genome duplication and mutations in *ACE2* cause multicellular, fast-sedimenting phenotypes in evolved *Saccharomyces cerevisiae*. Proc. Natl. Acad. Sci. USA 110: E4223–E4231.

Palecek, S. P., A. S. Parikh, and S. J. Kron, 2000 Genetic analysis reveals that *FLO11* upregulation and cell polarization independently regulate invasive growth in *Saccharomyces cerevisiae*. Genetics 156: 1005–1023.

Pan, X., D. S. Yuan, D. Xiang, X. Wang, S. Sookhai-Mahadeo *et al.*, 2004 A robust toolkit for functional profiling of the yeast genome. Mol. Cell 16: 487–496.

Payen, C., S. C. Di Rienzi, G. T. Ong, J. L. Pogachar, J. C. Sanchez *et al.*, 2014 The dynamics of diverse segmental amplifications in populations of *Saccharomyces cerevisiae* adapting to strong selection. G3 (Bethesda) 4: 399–409.

Poltak, S. R., and V. S. Cooper, 2011 Ecological succession in long-term experimentally evolved biofilms produces synergistic communities. ISME J. 5: 369–378.

Pringle, J. R., 1991 [52] Staining of bud scars and other cell wall chitin with Calcofluor, pp. 732–735 in *Methods in Enzymology 194–Guide to Yeast Genetics and Molecular Biology*. Academic Press, San Diego.

Ratcliff, W. C., R. F. Denison, M. Borrello, and M. Travisano, 2012 Experimental evolution of multicellularity. Proc. Natl. Acad. Sci. USA 109: 1595–1600.

Ratcliff, W. C., J. T. Pentz, and M. Travisano, 2013 Tempo and mode of multicellular adaptation in experimentally evolved *Saccharomyces cerevisiae*. Evolution 67: 1573–1581.

Ratcliff, W. C., J. D. Fankhauser, D. W. Rogers, D. Greig, and M. Travisano, 2015 Origins of multicellular evolvability in snowflake yeast. Nat. Commun. 6: 6102.

Renda, B. A., M. J. Hammerling, and J. E. Barrick, 2014 Engineering reduced evolutionary potential for synthetic biology. Mol. Biosyst. 10: 1668–1678.

Reynolds, T. B., and G. R. Fink, 2001 Bakers' yeast, a model for fungal biofilm formation. Science 291: 878–881.

Ribeiro, S. M., M. R. Felício, E. V. Boas, S. Gonçalves, F. Costa *et al.*, 2016 New frontiers for anti-biofilm drug development. Pharmacol. Ther. 160: 133–144.

Robinson, J. T., H. Thorvaldsdóttir, W. Winckler, M. Guttman, E. S. Lander *et al.*, 2011 Integrative genomics viewer. Nat. Biotechnol. 29: 24–26.

Roop, J. I., and R. B. Brem, 2013 Rare variants in hypermutable genes underlie common morphology and growth traits in wild *Saccharomyces paradoxus*. Genetics 195: 513–525.

Rothstein, R. J., and F. Sherman, 1980 Dependence on mating type for the overproduction of iso-2-cytochrome c in the yeast mutant *CYC7–H2*. Genetics 94: 891–898.

Ryan, O., R. S. Shapiro, C. F. Kurat, D. Mayhew, A. Baryshnikova *et al.*, 2012 Global gene deletion analysis exploring yeast filamentous growth. Science 337: 1353–1356.

Sanchez, M. R., A. W. Miller, I. Liachko, A. B. Sunshine, B. Lynch *et al.*, 2017 Differential paralog divergence modulates evolutionary outcomes in yeast. PLoS Genet. 13: e1006585.

Segrè, A. V., A. W. Murray, and J.-Y. Leu, 2006 High-resolution mutation mapping reveals parallel experimental evolution in yeast. PLoS Biol. 4: e256.

Servant, G., C. Pennetier, and P. Lesage, 2008 Remodeling yeast gene transcription by activating the Ty1 long terminal repeat retrotransposon under severe adenine deficiency. Mol. Cell. Biol. 28: 5543–5554.

Seshan, V. and A. Olshen, 2015 DNAcopy: a package for analyzing DNA copy data. Available at: https://bioconductor.org/packages/release/bioc/html/DNAcopy.html.

Shen, Y., X. Chen, B. Peng, L. Chen, J. Hou *et al.*, 2012 An efficient xylose-fermenting recombinant *Saccharomyces cerevisiae*. Appl. Microbiol. Biotechnol. 96: 1079–1091.

Sivakumar, G., D. R. Vail, J. Xu, D. M. Burner, J. O. Lay *et al.*, 2010 Bioethanol and biodiesel: alternative liquid fuels for future generations. Eng. Life Sci. 10: 8–18.

Smukalla, S., M. Caldara, N. Pochet, A. Beauvais, S. Guadagnini *et al.*, 2008 *FLO1* is a variable green beard gene that drives biofilm-like cooperation in budding yeast. Cell 135: 726–737.

Stark, H. C., D. Fugit, and D. B. Mowshowitz, 1980 Pleiotropic properties of a yeast mutant insensitive to catabolite repression. Genetics 94: 921–928.

Stratford, M., 1989 Yeast flocculation: calcium specificity. Yeast 5: 487–496.

Stratford, M., 1992 Lectin-mediated aggregation of yeasts—yeast flocculation. Biotechnol. Genet. Eng. Rev. 10: 283–342.

Sunshine, A. B., C. Payen, G. T. Ong, I. Liachko, K. M. Tan *et al.*, 2015 The fitness consequences of aneuploidy are driven by condition-dependent gene effects. PLoS Biol. 13: e1002155.

Taylor, M. B., and I. M. Ehrenreich, 2014 Genetic interactions involving five or more genes contribute to a complex trait in yeast. PLoS Genet. 10: e1004324.

Taylor, M. B., J. Phan, J. T. Lee, M. McCadden, and I. M. Ehrenreich, 2016 Diverse genetic architectures lead to the same cryptic phenotype in a yeast cross. Nat. Commun. 7: 11669.

Tenaillon, O., J. E. Barrick, N. Ribeck, D. E. Deatherage, J. L. Blanchard *et al.*, 2016 Tempo and mode of genome evolution in a 50,000-generation experiment. Nature 536: 165–170.

Teunissen, A. W., J. A. van den Berg, and H. Y. Steensma, 1995 Transcriptional regulation of flocculation genes in *Saccharomyces cerevisiae*. Yeast 11: 435–446.

Topiwala, H. H., and G. Hamer, 1971 Effect of wall growth in steady-state continuous cultures. Biotechnol. Bioeng. 13: 919–922.

Verstrepen, K. J., and F. M. Klis, 2006 Flocculation, adhesion and biofilm formation in yeasts. Mol. Microbiol. 60: 5–15.

Verstrepen, K. J., A. Jansen, F. Lewitter, and G. R. Fink, 2005 Intragenic tandem repeats generate functional variability. Nat. Genet. 37: 986–990.

Voordeckers, K., and K. J. Verstrepen, 2015 Experimental evolution of the model eukaryote *Saccharomyces cerevisiae* yields insight into the molecular mechanisms underlying adaptation. Curr. Opin. Microbiol. 28: 1–9.

Voth, W. P., A. E. Olsen, M. Sbia, K. H. Freedman, and D. J. Stillman, 2005 *ACE2*, *CBK1*, and *BUD4* in budding and cell separation. Eukaryot. Cell 4: 1018–1028.

Westman, J. O., and C. J. Franzén, 2015 Current progress in high cell density yeast bioprocesses for bioethanol production. Biotechnol. J. 10: 1185–1195.

Wilke, C. M., and J. Adams, 1992 Fitness effects of Ty transposition in *Saccharomyces cerevisiae*. Genetics 131: 31–42.

Williams, F. E., and R. J. Trumbly, 1990 Characterization of *TUP1*, a mediator of glucose repression in *Saccharomyces cerevisiae*. Mol. Cell. Biol. 10: 6500–6511.

Xu, H., and J. D. Boeke, 1991 Inhibition of Ty1 transposition by mating pheromones in *Saccharomyces cerevisiae*. Mol. Cell. Biol. 11: 2736–2743.

Yokobayashi, Y., R. Weiss, and F. H. Arnold, 2002 Directed evolution of a genetic circuit. Proc. Natl. Acad. Sci. USA 99: 16587–16591.

Zara, G., S. Zara, C. Pinna, S. Marceddu, and M. Budroni, 2009 *FLO11* gene length and transcriptional level affect biofilm-forming ability of wild flor strains of *Saccharomyces cerevisiae*. Microbiology 155: 3838–3846.

Zhang, S., T. Zhang, M. Yan, J. Ding, and J. Chen, 2014 Crystal structure of the WOPR-DNA complex and implications for Wor1 function in white-opaque switching of *Candida albicans*. Cell Res. 24: 1108–1120.

Zhang, Z., U. Varanasi, and R. J. Trumbly, 2002 Functional dissection of the global repressor Tup1 in yeast: dominant role of the C-terminal repression domain. Genetics 161: 957–969.

Zhou, H., J. Cheng, B. L. Wang, G. R. Fink, and G. Stephanopoulos, 2012 Xylose isomerase overexpression along with engineering of the pentose phosphate pathway and evolutionary engineering enable rapid xylose utilization and ethanol production by *Saccharomyces cerevisiae*. Metab. Eng. 14: 611–622.

Zordan, R. E., D. J. Galgoczy, and A. D. Johnson, 2006 Epigenetic properties of white–opaque switching in *Candida albicans* are based on a self-sustaining transcriptional feedback loop. Proc. Natl. Acad. Sci. USA 103: 12807–12812.

Communicating editor: A. Murray